

Engineering RGB color vision into *Escherichia coli*

Jesus Fernandez-Rodriguez^{1,2}, Felix Moser^{1,2}, Miryoung Song¹ & Christopher A Voigt^{1*}

Optogenetic tools use colored light to rapidly control gene expression in space and time. We designed a genetically encoded system that gives *Escherichia coli* the ability to distinguish between red, green, and blue (RGB) light and respond by changing gene expression. We use this system to produce 'color photographs' on bacterial culture plates by controlling pigment production and to redirect metabolic flux by expressing CRISPRi guide RNAs.

The RGB system is a synthetic 18-gene, 46-kilobase-pair genetic program that was abstracted into four subsystems to aid its implementation (Fig. 1a). First, the 'sensor array' combines the light sensors, which receive environmental signals^{1,2}. Second, the 'circuit' processes these signals, for example, to integrate them or to execute a dynamic response. Third, a 'resource allocator' connects the circuit output to actuators³. Finally, 'actuators' implement the biological functions that are the outputs of the circuit. Dividing the project into these subsystems allows each one to be designed, built, and optimized in isolation before they are all combined.

The sensor array was constructed by combining light sensors that respond to different wavelengths. The red and green sensors are based on phytochromes, with phycocyanobilin (PCB) chromophores that are produced by a two-gene metabolic pathway (*pcyA* and *ho1*)^{4–6}. Red light is sensed by a chimeric histidine kinase (Cph8*) that is switched on by infrared (705 nm) light and off by red (650 nm) light⁵. This sensor was previously used to create black-and-white photographic images⁵. The green-light sensor is based on *Synechocystis* CcaSR, which is switched on by green (535 nm) light and off by far-red (672 nm) light^{7,8}. The blue-light sensor uses a chimeric histidine kinase (YF1) containing a flavin mononucleotide (FMN) chromophore that is switched off by 470 nm light and is on in its absence⁹. The red, green, and blue sensors had to be redesigned to optimize their dynamic ranges when carried on one plasmid and achieve 10-fold repression⁵, 7-fold induction, and 15-fold repression, respectively, in response to their corresponding colors (Supplementary Results, Supplementary Figs. 1–4).

To activate gene expression, the signals from the red- and blue-light sensors need to be inverted, which is done by connecting them to NOT gates. In each NOT gate, the input promoter drives the expression of a repressor (CI or PhIF, respectively) that turns off the output promoter (Fig. 1b)^{8,10}. These circuits were optimized by lowering repressor expression to reduce toxicity and by mutating the CI output promoter to increase dynamic range (Online Methods). The inverted red- and blue-light sensors generate 16-fold and 25-fold induction, respectively, in response to appropriately colored light (Supplementary Fig. 2). The circuit layer offers the possibility to implement more complex signal processing—for example, pattern recognition or edge detection¹¹.

Following circuit processing, red-, green-, and blue-light signals induce the P_{λ} , $P_{\text{CpCG2-172}}$, and P_{PhIF} promoters, respectively. These promoters are connected to the expression of actuators via a resource-allocation system³. This technique modularizes the

system, enabling different actuators to be easily connected to the circuit outputs. The resource allocator is based on a split-phage RNA polymerase (RNAP) system in which a non-active 'core' fragment (650 residues) is expressed by a constitutive promoter (J23105). This core is then directed to three promoters by expressing smaller (331 residue) 'sigma' fragments that contain the DNA-binding domain. We selected the three sigma fragments (σ_{KIP} , σ_{CGG} , and σ_{T3}) that exhibited the least crosstalk. Additional partial substitution was performed, including the addition of ribozyme-based insulators (BydvJ and RiboJ)^{12,13}. After the incorporation of resource allocation, red, green, and blue light induce the P_{KIP} , P_{CGG} , and P_{T3} promoters 20-fold, 9-fold, and 41-fold, respectively (Supplementary Fig. 3).

Several design challenges complicated the construction of the complete RGB system. One concern was the re-use of parts, which can lead to homologous recombination¹⁴. The desirability of avoiding this motivated the decision to combine genes into operons, shuffle the codons of two of the sigmas, and diversify the terminators. In total, 18 strong synthetic terminators were used¹⁵. The complete design of the RGB system consists of 14 cistrons divided among four plasmids. This required changing the ribosome binding sites (RBSs), to balance expression, and changing the plasmid origins (Supplementary Fig. 4). Despite the size and number of plasmids, the use of T7 RNAP, and the number of regulators, there was no reduction in the final optical density at 600 nm (OD_{600}) of the cultures compared to that in empty vector controls (Supplementary Fig. 5).

The spectral response of the complete RGB system was measured using fluorescent reporters and flow cytometry (Fig. 1c,d; Supplementary Fig. 6). There is little spectral overlap between the three systems, and the peaks of the responses correspond to those expected from each sensor. As a control, each light sensor was knocked out, and this abrogated the response to the corresponding wavelength (Fig. 1e; Supplementary Fig. 7).

The fluorescent proteins were then replaced with enzymes that would generate colored pigments on a plate. Red, green, and blue colors were produced by expressing glucuronidase (GusA), β -galactosidase (LacZ), and *Methylophaga* flavin-containing monooxygenase (bFMO), respectively. To improve the dynamic range of green-color production from LacZ, we added the *ssrA* protease tag to LacZ (Supplementary Fig. 8). The native *gus* operon in the genome was modified with the J23115 promoter to constitutively express GusBC (Online Methods; Fig. 1b). RBS libraries were built for all three enzymes, and variants that generated the largest dynamic range were selected (Supplementary Fig. 9).

The ability to record a color picture was tested by adding 1 mg/ml tryptophan, 1 mM Rose-gluc, and 0.25 mM X-gal to an LB-agarose plate (Supplementary Note). The RGB color strain was spread onto this agarose plate, and a color image was projected onto the plate for 18 h. The products of each enzyme reaction rapidly form insoluble precipitates, permanently coloring the plate (Fig. 1a). This results in high-resolution color pictures (Fig. 2; Supplementary Figs. 10 and 11).

¹Synthetic Biology Center, Department of Biological Engineering, Massachusetts Institute of Technology, Cambridge, Massachusetts, USA. ²These authors contributed equally to this work. *e-mail: cvoigt@gmail.com

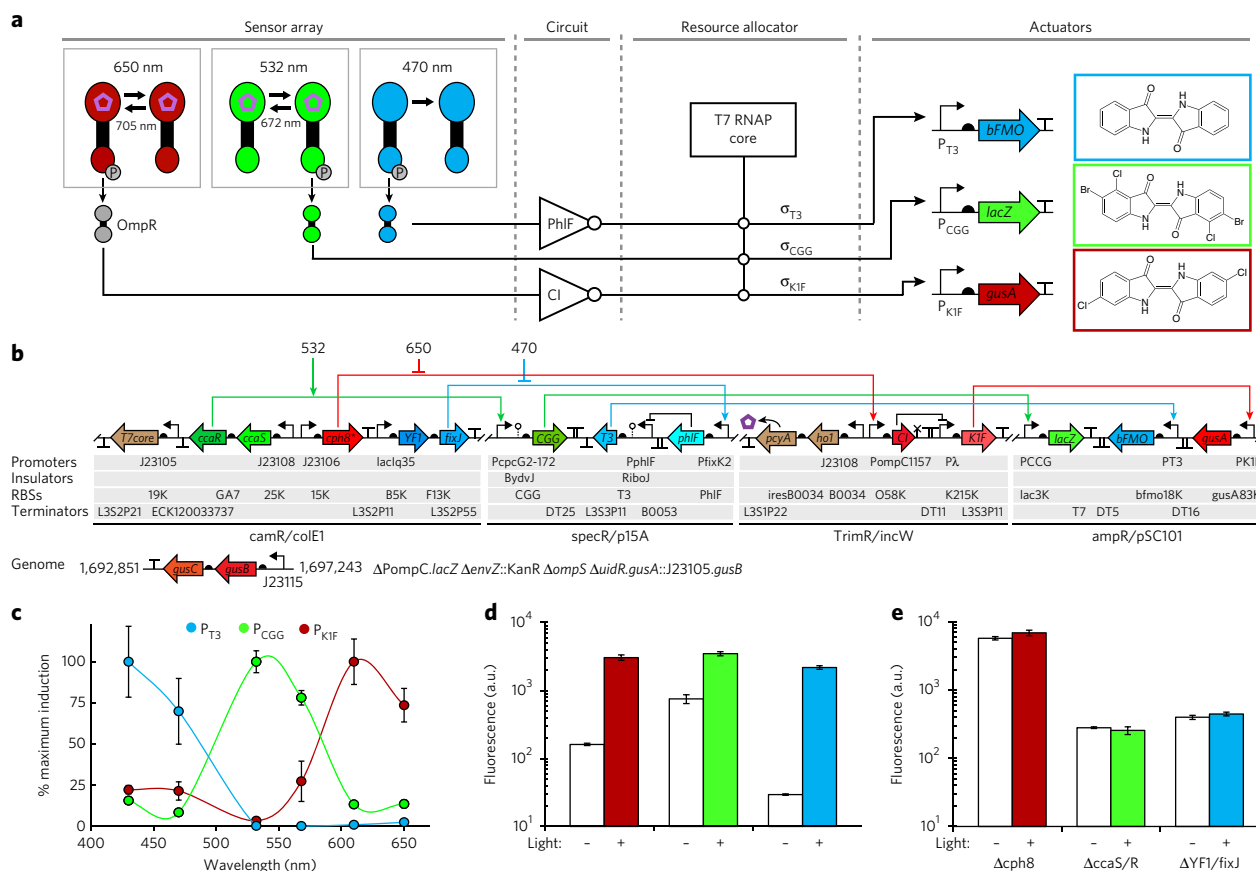


Figure 1 | The RGB system in *Escherichia coli*. (a) The design is composed of four subsystems, listed above. The final pigment compounds produced by each enzyme are shown. (b) The system is encoded on four plasmids and in the genome (**Supplementary Fig. 13**). OmpR, the response regulator phosphorylated by the red-light sensor histidine kinase Cph8*, is expressed from its native locus in the *E. coli* genome. The genes (arrows) and genetic parts are shown (**Supplementary Table 1**). (c) The spectral response of the complete RGB system. The outputs of the system are RFP, GFP, and BFP (**Supplementary Fig. 11**). “% maximum induction” is calculated as the fold change of the response divided by the maximum fold change across the spectrum. (d) The induction of the RGB strain with fluorescent reporters under 650 nm (red), 532 nm (green), or 470 nm (blue) light, showing the fluorescence of RFP, GFP, and BFP, respectively. Empty and colored bars indicate the absence and presence of light, respectively. (e) The same experiment as in d except that the individual sensors indicated were deleted from the plasmids. a.u., arbitrary units. The cytometry data for c and d, e are shown in **Supplementary Figures 6** and **7**, respectively. All error bars are the s.d. of three independent experiments done on different days.

When the RGB system is used to control the expression of fluorescent proteins, the image cannot be seen by eye alone but can be visualized using fluorescence microscopy (**Supplementary Fig. 12**).

One application of the RGB system is to implement feedback so that different colors of light can control flux through a metabolic pathway. We demonstrate this approach in *E. coli* by controlling the

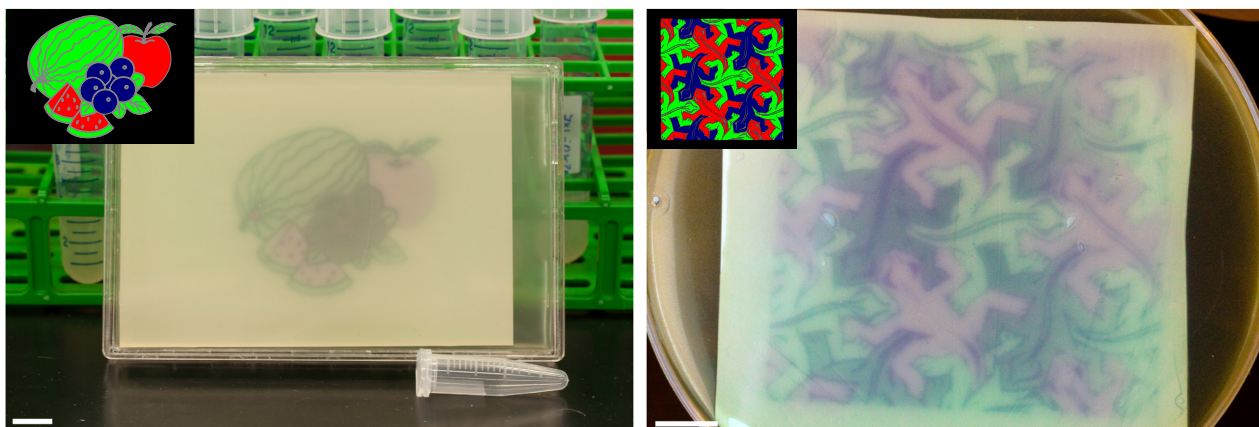


Figure 2 | Color photography by *Escherichia coli*. Colored images (insets) were projected onto plates of bacteria containing the RGB system. The resulting patterns of pigment are shown. An additional image is shown in **Supplementary Figure 11**. Higher-resolution images and a detailed guide to generating bacterial color photography are provided in the **Supplementary Figure 10**. Scale bars, 1 cm.

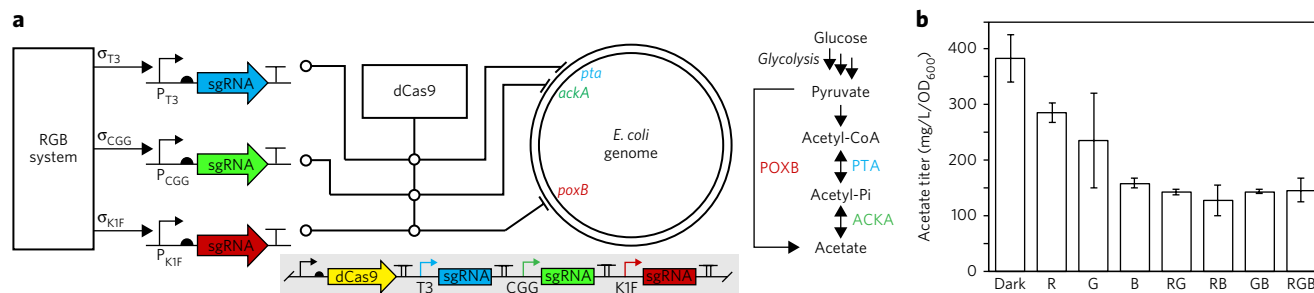


Figure 3 | Three-color control of metabolic flux to acetate. (a) Shown is the RGB system expressing CRISPR interference (CRISPRi) sgRNAs targeting the three genes in central carbon metabolism that control acetate production (*pta*, *ackA*, and *poxB*). (b) The titer of acetate is shown when cells are grown in red (R), green (G), or blue (B) light or in combinations thereof. Assay conditions and analytical techniques are provided in Online Methods. The final OD₆₀₀ of the cultures are shown in **Supplementary Figure 5**. Error bars are one s.d. of three independent experiments done on different days.

flux to acetate, which is a common byproduct of bio-processes¹⁶. Here, we use CRISPR interference (CRISPRi)¹⁷ to regulate the three endogenous genes that lead to acetate production (*pta*, *ackA*, and *poxB*) by designing single-guide RNAs (sgRNAs) that target each gene (Online Methods). Each sgRNA was placed under the control of the red-, green-, and blue-light-activated promoters P_{KIF} , P_{CGG} , and P_{T3} , respectively (Fig. 3a). Catalytically inactivated dCas9 is expressed constitutively at a low level. Individually and in combination with one another, the different colors of light reduce acetate production without sacrificing biomass accumulation (Fig. 3b; **Supplementary Fig. 5**).

In 2005, we built a strain of *E. coli* that can record black-and-white images⁵. This design was representative of the complexity that could be achieved in the field at the time¹⁸, requiring only four genes and three promoters. By contrast, the RGB color system is large and multifaceted, consisting of 18 genes, 14 promoters, 18 terminators, and 4 plasmids, totaling 46,198 base pairs of DNA. The success of this system required advances to reliably integrate sensing, regulation, resource usage, and metabolism and to physically construct the system. These developments include libraries of characterized genetic parts and orthogonal regulators, methods to tune expression, insulation of context effects, reduction of evolutionary fragility, and CRISPRi for the control of native genes.

Colored light offers many channels to pattern cells to build tissues or materials, control cells at a distance, or serve as a means of communication between electronic and biological systems. In nature, single cells can contain dozens of light sensors that respond to the rainbow of colors as well as near-UV and far-infrared (IR)¹⁹ light, and these have been applied to eukaryotes and animals^{20,21}. Individually, these light sensors have been used to remotely control pathways in a bioreactor²², induce lysis^{23,24}, and implement genome editing²⁵, and also have biomedical applications². Fully harnessing the spectral range of light sensors simultaneously in individual cells provides many knobs by which cells can be controlled rapidly and spatially and from afar.

Received 19 July 2016; accepted 3 March 2017;
published online 22 May 2017

Methods

Methods, including statements of data availability and any associated accession codes and references, are available in the [online version of the paper](#).

References

- Deisseroth, K. *Nat. Methods* **8**, 26–29 (2011).
- Bacchus, W. & Fussenecker, M. *Curr. Opin. Biotechnol.* **23**, 695–702 (2012).

- Segall-Shapiro, T.H., Meyer, A.J., Ellington, A.D., Sontag, E.D. & Voigt, C.A.A. *Mol. Syst. Biol.* **10**, 742 (2014).
- Gambetta, G.A. & Lagarias, J.C. *Proc. Natl. Acad. Sci. USA* **98**, 10566–10571 (2001).
- Levskaya, A. *et al. Nature* **438**, 441–442 (2005).
- Rockwell, N.C. & Lagarias, J.C. *ChemPhysChem* **11**, 1172–1180 (2010).
- Hirose, Y., Shimada, T., Narikawa, R., Katayama, M. & Ikeuchi, M. *Proc. Natl. Acad. Sci. USA* **105**, 9528–9533 (2008).
- Tabor, J.J., Levskaya, A. & Voigt, C.A. *J. Mol. Biol.* **405**, 315–324 (2011).
- Möglich, A., Ayers, R.A. & Moffat, K. *J. Mol. Biol.* **385**, 1433–1444 (2009).
- Stanton, B.C. *et al. Nat. Chem. Biol.* **10**, 99–105 (2014).
- Tabor, J.J. *et al. Cell* **137**, 1272–1281 (2009).
- Lou, C., Stanton, B., Chen, Y.J., Munsky, B. & Voigt, C.A. *Nat. Biotechnol.* **30**, 1137–1142 (2012).
- Nielsen, A.A. *et al. Science* **352**, aac7341 (2016).
- Sleight, S.C., Bartley, B.A., Lieviant, J.A. & Sauro, H.M. *J. Biol. Eng.* **4**, 12 (2010).
- Chen, Y.J. *et al. Nat. Methods* **10**, 659–664 (2013).
- De Mey, M., De Maeseneire, S., Soetaert, W. & Vandamme, E. *J. Ind. Microbiol. Biotechnol.* **34**, 689–700 (2007).
- Qi, L.S. *et al. Cell* **152**, 1173–1183 (2013).
- Purnick, P.E. & Weiss, R. *Nat. Rev. Mol. Cell Biol.* **10**, 410–422 (2009).
- Rockwell, N.C. *et al. Proc. Natl. Acad. Sci. USA* **111**, 3871–3876 (2014).
- Shimizu-Sato, S., Huq, E., Tepperman, J.M. & Quail, P.H. *Nat. Biotechnol.* **20**, 1041–1044 (2002).
- Buckley, C.E. *et al. Dev. Cell* **36**, 117–126 (2016).
- Lee, J.M., Lee, J., Kim, T. & Lee, S.K. *PLoS One* **8**, e52382 (2013).
- Magaraci, M.S. *et al. ACS Synth. Biol.* **3**, 944–948 (2014).
- Miyake, K. *et al. Biotechnol. Biofuels* **7**, 56 (2014).
- Farzadfard, F. & Lu, T.K. *Science* **346**, 1256272 (2014).

Acknowledgments

The authors would like to thank N. DeLateur and R. Weiss for assistance with fluorescence microscopy and L. Gonzalez for assistance with hardware. This work was supported by US National Science Foundation Synthetic Biology Engineering Research Center (SynBERC EEC0540879), the Office of Naval Research Multidisciplinary University Research Initiative (N00014-11-1-0725 and N00014-13-1-0074), and the National Institutes of Health (R01-GM095765 and R01-GM096164).

Author contributions

C.A.V., J.F.-R., and F.M. conceived of the study and designed the experiments. J.F.-R. and F.M. performed the experiments and analyzed the data. M.S. designed and built the genomic *gusBC* system. C.A.V., J.F.-R., and F.M. wrote the manuscript.

Competing financial interests

The authors declare no competing financial interest.

Additional information

Any supplementary information, chemical compound information and source data are available in the [online version of the paper](#). Reprints and permissions information is available online at <http://www.nature.com/reprints/index.html>. Publisher's note: Springer Nature remains neutral with regard to jurisdictional claims in published maps and institutional affiliations. Correspondence and requests for materials should be addressed to C.A.V.

ONLINE METHODS

Strains and media. The strain *Escherichia coli* JT2 was used for the RGB fluorescence output systems. *E. coli* JT2 is a derivative of *E. coli* RU1012 (MC4100 ara+ Δ (OmpC-lacZ) 10-25 Δ envZ::Kan^R) that contains a deletion of the P_{ompC} -lacZ region as previously described^{8,11}. The strain *E. coli* JF1 was used for the colored pigment output systems. To construct *E. coli* JF1, the native genes *uidR* and *gusA* were replaced with a promoter that constitutively expressed the native genes *gusBC*. In this operon, a single point mutation in *gusB* was reverted to a working variant (L100P). To do this, the *gusBC* operon under control of the constitutive J23115 promoter was cloned adjacent to a chloramphenicol resistance marker (*camR*) flanked by FLP recombinase sites in a pSC101 plasmid. From this vector, the DNA cassette including the *camR* gene and J23115 driving *gusB* was amplified by PCR, purified, and transformed into JT2 expressing lambda-red recombinase²⁶. Following insertion by homologous recombination, *camR* was removed by FLP recombinase expressed from the plasmid pCP20. The final *gusBC* genomic locus was sequence verified by colony PCR and subsequent Sanger sequencing (Quintara). All cultures were grown in LB medium (BD # 2020-05-31) unless otherwise indicated. The industrial minimal media used in the acetate production cultures contained 5 g/L (NH₄)₂SO₄ (EMD #AX1385-1), 5 g/L K₂HPO₄ (VWR #0705), 30 g/L MES (Sigma #M2933), 16 g/L glucose (BDH #8005-500g), and a proprietary mixture of micronutrients as previously described²⁷, and its pH was brought to 6.8 with NaOH and HCl. Antibiotics were added at the following concentrations to maintain plasmids in all liquid cultures and plates: 50 µg/ml kanamycin (GoldBio; #25389-94-0), 100 µg/ml spectinomycin (GoldBio; #22189-32-8), 100 µg/ml ampicillin (GoldBio; #69-52-3), 35 µg/ml chloramphenicol (AlfaAesar; #25-75-7), and 10 µg/ml trimethoprim (Biomedical Inc.; #195527).

Liquid cultures in plates. For fluorescence assays, fresh cultures were inoculated from single colonies streaked from a glycerol stock frozen at -80 °C. Inoculum cultures were grown overnight in 3 ml of LB media at 37 °C in 15 ml culture tubes (Falcon, #352059), wrapped in aluminum foil to prevent ambient-light exposure for 18 h. The culture was then diluted 1/100 into 800 µl of fresh LB media containing antibiotics in a 2 ml deep-well 96-well plate (USA Scientific, #1896-2000). Following inoculation, the plate was covered with a transparent Breathe-Easy membrane (USA Scientific, #9123-6100). Two plates were prepared identically. One plate was then placed in a cardboard box, keeping it dark. This plate is the “dark” plate listed below. The second plate was exposed to light as described and is the “light” plate described below. The “light” and “dark” plates were taped to the surface of a shaker (VWR, #97043-608) placed inside an incubator set to 37 °C and shaken at 800 r.p.m. for 8 h before analysis. Light was shined into the incubator through a 5-cm diameter hole in the top of the incubator 43 cm above the plate. The light source was a slide projector (Kodak Ektagraphics III) containing a 300-Watt white light bulb (Divine Lighting). We used an identical setup as the one described previously²⁸. The following optical band pass filters (25 mm diameter; Edmund optics) were used to filter different colors from the white light source: 430 nm (#65-682), 470 nm (#65-689), 532 nm (#65-700), 568 nm (#65-705), 632 nm (#65-711), and 650 nm (#65-715). Neutral density filters (Edmund optics, #49-066) were used to adjust the intensity of the incident light. We used a SpectraWiz spectrometer (StellarNet) to measure the intensity of the incident light (200 ms integration time) at each respective wavelength above as follows: 1.5 W/m² for 430 nm, 2.8 W/m² for 470 nm, 11.7 W/m² for 532 nm, 15.3 W/m² for 568 nm, 24.5 W/m² for 632 nm, and 11.1 W/m² for 650 nm. These intensities were used for screening assays as well as for the spectral data in **Figure 1c**.

Liquid cultures in tubes. For the acetate experiments, we built a hardware system that enabled us to expose bacteria grown in 15 ml culture tubes to three LED light inputs that is similar to hardware developed by Tabor and co-workers²⁹. In our system, we removed the tip of a 50 ml Falcon tube and inserted custom three-dimensional-printed plastic parts that secured a 15-ml tube in place and enabled insertion of three 5-mm LEDs near the bottom of the tube. Red (630 nm, 16° viewing angle, 20 mA, Cree #C503B-RCN-CW0Z0AA1), green (525 nm, 60° viewing angle, 20 mA, Kingbright #WP7083ZGD), and blue (472 nm, 60° viewing angle, 20 mA, Multicomp #MCL053SBL) LEDs were inserted into these holes and wired to an Arduino Mega 2560 circuit board. By programming the

analog outputs of the circuit board, we scanned a range of each LED's intensity for the intensity that produced maximum activation of each respective sensor. Red, green, and blue LED intensity was therefore set to 8.9 W/m², 8.1 W/m², and 4.6 W/m², respectively. Each 50-ml container module was wrapped in aluminum foil to prevent light contamination and placed in a rack in an Innova 44 incubator (New Brunswick Scientific). This ‘light rack’ setup could hold up to 20 tubes at once and was easily scalable. The Arduino board and wires were fixed to the floor of the incubator next to the light rack. For tube growth assays, cells carrying the RGB plasmids pJFR1, pJFR2, pJFR3, and output plasmid pFM1192 were freshly streaked from a -80 °C glycerol stock and grown overnight on LB media containing antibiotics in light-insulated tubes as described above. Cells were diluted 1/1,000 from the overnight culture into 3 ml of minimal media containing antibiotics and 1.6% glucose in 15 ml culture tubes. Cultures were then placed in the light rack and shaken at 250 r.p.m. at 37 °C for 48 h. For all light-rack assays, cells were exposed to either no light or every single, double, and triple combination of red, green, and blue LED light. Supernatants were harvested by centrifuging an initial 2 ml of culture at 15,000 r.p.m. for 5 min three times, taking half the supernatant after each spin.

Liquid chromatography. To assay the acetate titer in culture supernatants, we used an Agilent 1260 Infinity Liquid Chromatography system with an inline Aminex HPX-87H column (Bio-Rad, CA, 125-0140) and Micro-Guard Cation column (Bio-Rad, CA, 125-0129) running a 5-mM sulfuric acid mobile phase at a flow rate of 0.6 ml/min. For the assay, we pipetted 100 µl of supernatant into the bottom of a U-bottom 96-well plate (Corning, ME, 3797), covered the plate with an AluminaSeal (Diversified Biotech, MA; ALUM-1000), and placed the plate in an autosampler cooled to 4 °C. The autosampler injected 10 µl of each sample for analysis, with a 3-s isopropanol rinse of the needle between sampling. A refractive index detector (RID; Agilent; G1362A) was used to quantify the peak for acetate (15.5 min). Both the columns and the RID were heated to 35 °C. Standard curves of acetate (Fluka; #57191) were run with each assay to enable accurate quantification. Integration of the RI peaks for acetate was done automatically in ChemStation software (Agilent).

Flow cytometry. Cells were analyzed by flow cytometry on an LSR Fortessa analyzer (BD Biosciences). RFP, GFP, and BFP fluorescence was measured using a 561-nm laser and 610/20 nm band pass filter, a 488-nm laser and 510/20 nm band pass filter, and a 405-nm laser and 450/50 nm band pass filter, respectively. Sampled cells were diluted 1/100 into cold phosphate-buffered saline (pH = 7) containing 1 g/L kanamycin to arrest translation. Cells were then left at 4 °C for 1 h before measurement to allow all fluorescent proteins to fold. Samples of 10 µl were run at 0.5 µl/s until 10⁴–10⁵ events were collected. FSC-H and SSC-H thresholds were set to exclude background events. Data was analyzed using FlowJo software (Tree Star). The median of the fluorescence histogram of each gated population was calculated and is reported here as the fluorescence value of a sample in arbitrary units (a.u.).

Fluorescence microscopy. Photographic plates of the RGB system controlling fluorescent proteins (pJFR1, pJFR2, pJFR3, and pJFR4) were generated as detailed in the **Supplementary Note**. To image the resulting fluorescent protein pattern, we imaged RFP, GFP, and BFP fluorescence channels with a Zeiss Axiovert 200M microscope using a 1.25× objective. The RFP channel used an excitation source of 565/30 nm and collected emission with a 620/60 nm filter (Zeiss #000000-1031-350). The GFP channel used an excitation source of 470/40 nm and collected emission with a 525/50 nm filter (Zeiss #000000-1031-346). The BFP channel used an excitation source of 390/22 nm and collected emission with a 460/50 nm filter (Zeiss #000000-1031-334). To generate an image of the entire pattern, an 8 × 8 grid of 0.5 × 0.7 mm fields were collected in each channel and stitched together in the AxioVision (Zeiss) software.

Optimization of the red-light sensor. We previously reported a Cph8 red-light sensor that repressed *lacZ* expression ~10-fold in response to 650 nm light compared to dark conditions⁵. Tabor and co-workers improved the dynamic range of this system to 19-fold by using a synthetic promoter (J23106) and RBS to constitutively express a more active G722V variant of Cph8 (termed Cph8*) and a truncated version of the P_{ompC} output promoter ($P_{ompC1157}$)³⁰. We cloned

this constitutive *cph8** gene onto a *colE1* plasmid to generate the sensor plasmid pRED (Supplementary Fig. 2). Both the Cph8* (red) and CcaS (green) sensors require phycocyanobilin (PCB) to function. PCB is synthesized by the genes *pcyA* and *ho1*. Tabor and co-workers optimized polycistronic expression of *pcyA* and *ho1* by constitutively expressing the genes from the synthetic promoter J23108 on a p15A plasmid. We built a similar construct to produce PCB and to serve as a reporter, expressing GFP from the cognate sensor promoter. To create a system that activates instead of repressing in response to 650 nm light, we previously engineered a red-light sensor coupled to a NOT gate (CI repressor) to generate a circuit that induced *lacZ* by 2.5-fold in response to 650 nm light⁸. Similarly, we cloned the P_{ompc1157} promoter upstream of CI and a strong double terminator on a p15A plasmid. This expression cassette is followed by a P_λ promoter (R0065) driving GFP expression (www.partregistry.org). We called this final measurement plasmid pOmpc-CI (Supplementary Fig. 2). *E. coli* JT2 cells were co-transformed with pRED and pOmpc-CI to test their activity under 650 nm red light. Initially, we observed substantial toxicity that impeded measurement. To mitigate this toxicity, we created a RBS library for CI (See section “RBS library design and screening”). This approach yielded a system that produced a 16-fold change in fluorescence between the light (650 nm) and dark states (Supplementary Fig. 2). During screening of the RBS library for K1F, we isolated a variant of P_λ with a 16-base-pair deletion that eliminated a putative −10 site and increased the dynamic range of the response to 25-fold. We used this P_λ variant for the final RGB system.

Optimization of the green-light sensor. We previously reported a green-light sensor based on the *ccaS/R* genes from the cyanobacterium *Synechocystis* that induced *lacZ* expression by two-fold in response to 532 nm green light compared to dark conditions⁸. Tabor and co-workers obtained >100-fold induction of GFP in green compared to red conditions by tuning the RBS strengths of constitutively transcribed *ccaS* and *ccaR* on two separate plasmids and implementing an improved P_{cpcG2-172} output promoter³⁰. We chose to express both *ccaS* and *ccaR* from the same constitutive promoter J23106 on a *colE1* origin plasmid, referred to as pGREEN (Supplementary Fig. 1). We constructed a reporter plasmid encoding the PCB pathway and the *gfp* gene under the control of the engineered P_{cpcG2-172} promoter on a p15A plasmid, referred to as pCpcG2-GFP (Supplementary Fig. 1). We created an RBS library for *ccaR* in the first instance of pGREEN. We describe the design and creation of this library in detail below. Briefly, we co-transformed JT2 cells with the pGREEN library and pCpcG2-GFP and screened the resulting strains for GFP production under 532 nm light (See section “RBS library design and screening”). We isolated a variant showing seven-fold induction of GFP in response to green light compared to that in dark conditions (Supplementary Fig. 1).

Optimization of the blue-light sensor. We cloned the YF1 and FixJ sequences³¹ into a *colE1* plasmid, pBLUE (Supplementary Figs. 1 and 2). We initially implemented a NOT gate based on the transcriptional repressor SrpR¹⁰. The P_{fixK2} promoter was cloned upstream of SrpR and a strong double terminator on a p15A plasmid. Downstream of this expression cassette, we cloned the P_{SrpR} promoter driving a GFP output (pFix-SrpR). We co-transformed *E. coli* JT2 cells with pBLUE and pFix-SrpR to test their capacity to activate GFP expression under blue light (470 nm). However, this strain showed an extreme growth defect and could not be measured. We hypothesized that this defect was due to SrpR overexpression. To mitigate toxicity, we fused an *ssrA*-LVA tag onto SrpR to reduce the half-life of the repressor. The resulting strain showed a 25-fold induction of GFP when exposed to 470 nm light compared to growth in the dark. Subsequently, we replaced the SrpR repressor with the PhlF repressor to reduce crosstalk between SrpR and P_λ, which contained a putative SrpR binding site (Supplementary Fig. 4).

RBS library design and screening. RBS library sequences were computationally generated using the RBS Library Calculator tool (Version 1.1)³². Each library contained at least 50 member RBS sequences that evenly spanned 2–3 orders of magnitude in calculated strength (a.u.). These sequences were then integrated into primers for amplification of the target plasmid. RBS libraries were constructed using iPCR, in which directly adjacent, diverging primers encoding the library at their 5′ ends were used to amplify a plasmid. The resulting PCR product was purified with a PCR purification kit (Zymo) and incubated for 12 h with T4 polynucleotide kinase (NEB# M0201S) and T4 DNA ligase (NEB #M0202T) at 16 °C. The resulting ligation was transformed directly into the appropriate screening strain.

To generate *ccaR* RBS library, the primers JFR1097 (TCTTAGRAGSWC CATAGATGAGAATTCTTTTAGTGAGGATGATTTGCCGCTGG CGG) and JFR1098 (AGAGATATATCTATCTCTTATTACTAAGCTCGAGG CAAATGGTTATAGCGTTTAAAC) were used to amplify pGREEN. The purified *ccaR* RBS library was transformed into *E. coli* JT2 cells carrying the reporter pCpcG2-GFP and plated on LB agar containing chloramphenicol and spectinomycin. Similarly, the CI repressor RBS library was generated using primers JFR1032 (MYTACTAAAGACAGAGGAGRGTTACACT ATGAGCACAAAAAGAAACCATTAAACAAGA) and JFR1033 (CGG GCAGATTCCCCCTCGTGCTTCAAAATATC) to amplify pOmpC-CI. The purified CI RBS library was transformed into *E. coli* JT2 cells carrying the reporter pRED and plated on LB agar containing chloramphenicol and trimethoprim. For each library, 96 colonies of transformants were picked into 500 µl of LB medium containing the appropriate antibiotics in a 96-well deep-well plate and grown to saturation in the dark for 18 h. The next day, liquid culture assays were performed as described above. Briefly, 1 µl of cells from each well was added to 800 µl of LB in a 96-well deep-well plate, and the plate was covered with a transparent BreathEasy membrane (USA Scientific, #9123-6100). Two plates were prepared identically. One plate was then placed in a cardboard box to protect it from light and the other was exposed to light filtered by band-pass filters. For the *ccaR* RBS library, a 532 nm band pass filter was used. For the CI RBS library, a 650-nm band pass filter was used. Cultures were grown for 8 h and then measured by flow cytometry as described. The cultures that showed the biggest fold-change in GFP fluorescence were streaked and the RBS locus was sequenced.

Growth measurements. Cells carrying either empty vectors (pFM1064, pFM1065, pFM1066, and pFM1067) or all the RGB plasmids (pJFR1, pJFR2, pJFR3, and pJFR5) were grown for 18 h in LB media containing antibiotics as described above. Cells were then diluted 1/100 into 200 µl of LB media containing antibiotics in a clear-bottom 96-well plate (Nunc), the plate was covered with a BreathEasy membrane, and the plate was placed in a plate reader (BioTek Synergy H1). Cells were shaken at 600 RPM between absorbance measurements. Reported is the final OD₆₀₀ after 18 h.

Data availability. Data generated or analyzed during this study are included in this published article (and its supplementary information files) or are available from the corresponding author upon reasonable request.

26. Datsenko, K.A. & Wanner, B.L. *Proc. Natl. Acad. Sci. USA* **97**, 6640–6645 (2000).

27. Moser, F. *et al. ACS Synth. Biol.* **1**, 555–564 (2012).

28. Tabor, J.J. *Methods Enzymol.* **497**, 373–391 (2011).

29. Gerhardt, K.P. *et al. Sci. Rep.* **6**, 35363 (2016).

30. Schmidl, S.R., Sheth, R.U., Wu, A. & Tabor, J.J. *ACS Synth. Biol.* **3**, 820–831 (2014).

31. Ohlendorf, R., Vidavski, R.R., Eldar, A., Moffat, K. & Möglich, A. *J. Mol. Biol.* **416**, 534–542 (2012).

32. Tian, T. & Salis, H.M. *Nucleic Acids Res.* **43**, 7137–7151 (2015).